Center for Turbulence Research
Proceedings of the Summer Program 2004

Hartmann effect on MHD turbulence in the limit $Rm \ll 1$

By B. Knaepen†, Y. Dubief AND R. Moreau‡

This work is an attempt to model the actual MHD flows at the laboratory scale ($Rm \ll 1$). It essentially focuses on how to take into account the influence of the Hartmann layers on the turbulence present in the core flow, namely when the applied magnetic field is large enough to impose a quasi-2D regime. The model studied is obtained from the classical theory of Hartmann layers and consists in extra damping terms in the evolution equation of the fluid. Numerical results show that the model predicts the expected behavior of the core flow between Hartmann layers. A striking property is however that the component of the velocity field parallel to the magnetic field does not evolve to an anisotropic state as observed for the perpendicular components. This behavior is supported by an analytical analysis.

1. Introduction

Most of the experiments on MHD achievable at the laboratory scale concern fluids, such as liquid metals, whose magnetic diffusivity $\eta = 1/(\mu\sigma)$ (μ stands for their magnetic permeability and σ for their electrical conductivity) is extremely large in comparison with their kinematic viscosity ν. This implies that the magnetic Reynolds number $R_m = UL/\eta$ (U is a typical velocity scale, L a typical length scale) is often much smaller than unity (typically in the range 10^{-4}-10^{-2}), whereas the ordinary Reynolds number $Re = UL/\nu$ is much larger than unity (typically in the range 10^3-10^5). As a consequence, the distribution of the magnetic field is controlled by diffusion, what means that the actual field is negligibly disturbed by the fluid flow. Then, the magnetic field may be considered as given, and in the following it is supposed uniform and denoted $\mathbf{B}$.

Many experiments have been performed in such conditions, first in Riga and in Purdue (see Lielausis 1975; Tsinober 1990) then in Beer-Sheva (Branover 1978) and in Grenoble (A. Alemany & Frisch 1979; Sommeria 1986; Messadek & Moreau 2002), which have provided a fairly good knowledge of the specific properties of this kind of MHD turbulence. The understanding of the mechanisms by which the magnetic field is influencing this turbulence has also received significant attention (A. Alemany & Frisch 1979; Sommeria & Moreau 1982; Davidson 1995, 1997). The numerical modeling of this kind of MHD turbulence has also started (Zikanov & Thess 1998; Lee & Choi 2001; Knaepen & Moin 2004) but the tools to compute such flows are still far from being capable to include all the majors effects of the magnetic field. It will be seen, later on, that one of the major properties of this MHD turbulence is to become quasi-two-dimensional (Q2D). Then, an inverse cascade of energy is substituted to the familiar direct cascade in ordinary turbulence. As a consequence, the relevant length scales are larger than in ordinary turbulence and the computation domain must also be larger, as well as the computation time. One

† Université Libre de Bruxelles, Brussels, Belgium
‡ Laboratoire EPM, ENSHMG, Grenoble, France

may also notice that the small scales become less relevant and expect that this kind of turbulence be particularly well adapted to large eddy simulations (LES).

This report is organized as follows. In section 2, the classical theory of Hartmann layers and their influence on the core flow are outlined. The main section of our report follows in section 3. The model describing the influence of the Hartmann layers on the core flow is formulated and numerical results testing its predictions are presented. The emphasis is put on the evolution of the kinetic energy of the flow and on the anisotropy that develops in the flow. We conclude this report in section 4 and highlight indicate lines of future research.

2. Basic ideas on the Hartmann damping

Among the effects of the magnetic field on the turbulence, the first one is the development of an anisotropy, which becomes quite pronounced when the magnetic field is very large. In the case of homogeneous turbulence, this anisotropy is particularly clear in the Fourier space, since the Fourier transform of the Lorentz force is depending on the direction of the wave vector, but independent of its magnitude (A. Alemany & Frisch 1979). Indeed, the energy carried by wave vectors parallel to $\mathbf{B}$ is rapidly damped out, in a time scale of the order of $\tau_J = \rho/(\sigma B^2)$ (ρ is density, τ_J is usually named the Joule time scale and B is the norm of $\mathbf{B}$), whereas the energy carried by wave vectors perpendicular to $\mathbf{B}$ is not directly damped by the Lorentz force. However, inertia is capable to withdraw some energy from these wave vectors perpendicular to $\mathbf{B}$ and to transfer it to wave vectors more rapidly damped. Such inertial transfer mechanisms, between wave vectors of similar magnitudes but different directions, are far from being well understood as they have not been the subject of as many investigations as the usual energy transfers between different wave numbers. What is generally accepted is that their time scale is still the eddy turnover time $\tau_{tu} = l/u$ (here l and u are length and velocity scales of turbulent eddies). And the net result of the competition between the Joule damping and inertia still leads to a time decay following a power law of the form t^{-n} with $n \approx 1.7$ instead of 1.1 or 1.2 in ordinary isotropic turbulence (A. Alemany & Frisch 1979).

There is another way to understand the development of this anisotropy, without using Fourier transforms and wave vectors, which has the advantage to be valid in non-homogeneous turbulence. It is based on the fact that, when $Rm \ll 1$, the well known Alfven waves degenerate into a diffusion along the magnetic field lines (Sommeria & Moreau 1982). Due to this mechanism, any initial eddy elongates in the direction parallel to $\mathbf{B}$ according to a law

$$\frac{l_\parallel}{l_\perp} \sim \left(\frac{\sigma B^2 t}{\rho}\right)^{\frac{1}{2}}. \tag{2.1}$$

So, substituting τ_{tu} instead of t, one may easily guess what the anisotropy of any given eddy may be during its life time. One should notice that eddies with significantly large $l_\perp$ may get a length scale $l_\parallel$ of the same order as or larger than the width of the whole domain h. Then, such eddies are column-like and one may say that this turbulence becomes Q2D, after a duration of the order of

$$\tau_{2D} = \tau_J \left(\frac{h}{l_\perp}\right)^2. \tag{2.2}$$

Other very important effects come from the influence of the Hartmann walls on the

turbulence. This influence is at least twofold. First, the presence of the walls just forces the velocity component perpendicular to them to be zero, because it cannot vary significantly through the thin Hartmann boundary layer. Then, within the Q2D columns, the velocity vectors tend to remain within planes perpendicular to the magnetic field. The second influence of the Hartmann walls has its origin in one of the striking properties of the Hartmann boundary layer, which is not a passive layer like the Blasius layer, but which is a primary layer, capable to react on the core flow. This property is the fact that a significant Joule damping remains present within the layer where the velocity cancels whereas the electric field $\mathbf{E}$ does not. As a consequence, the balance between $\mathbf{E}$ and $\mathbf{u} \times \mathbf{B}$, which is present in the core and minimizes the current density, is destroyed and the current density is locally very important (of the order of σBu, whereas it is Ha less within the core, $Ha = \sqrt{\sigma/(\rho\nu)}Bh$ being the Hartmann number built with the width between the Hartmann walls h). On this basis, Sommeria & Moreau (1982) have shown that the effective Joule damping time, which is then named the Hartmann time, is $\tau_H = Ha\tau_J = h/B\sqrt{\rho/(\sigma\nu)}$. It may be much larger than τ_J, since it varies as B^{-1} (not B^{-2} as τ_J).

3. Damping of the homogeneous core flow in a Hartmann channel

3.1. *Formulation*

Since the Hartmann layers are very thin (their thickness $\delta = B^{-1}\sqrt{\rho\nu/\sigma}$ may be around 30 μm in mercury with a magnetic field of 1 Tesla), the fluid velocity is uniform in the main part of the channel. Then, except in those layers where the shear is localized, the turbulence may be homogeneous. According to what was described in the former section, it is also Q2D as soon as τ_{2D} is significantly shorter than the eddy turn over time $\tau_{tu} = l_\perp/u_\perp$. Then the velocity component parallel to the magnetic field, which may be non-zero in the initial state, is submitted to a linear damping in a time scale of the order of τ_{2D}. This may be easily modeled with the addition of the term $-u_\parallel/\tau_{2D}$ in the right hand side of the equation for $u_\parallel$. The velocity components in the plane perpendicular to $\mathbf{B}$ are also affected by some damping, but much less rapidly, as explained in section 2. Indeed, they are only submitted to the Hartmann damping, which may be expressed by the addition of the term $-u_\perp/\tau_H$ in the right hand side of the equation for $u_\perp$. The damping force F_i associated with the Hartmann layers is therefore tentatively modeled by

$$F_x = -u_x/\tau_H,\ F_y = -u_y/\tau_H,\ F_z = -u_z/\tau_{2D}, \tag{3.1}$$

where the z-direction has been chosen as the wall-normal direction. The form 3.1 cannot be used as such since it would not respect the incompressibility of the flow. However it can easily be projected on its solenoidal part F_i^S. Using the Fourier representation, F_i^S can be written as

$$F_i^S = (\delta_{ij} - \frac{k_i k_j}{k^2})F_j. \tag{3.2}$$

Again in Fourier representation, the actual components of F_i^S are then,

$$F_x^S = -u_x/\tau_H + (1/\tau_{2D} - 1/\tau_H)\frac{k_x k_z}{k^2}u_z \tag{3.3}$$

$$F_y^S = -u_y/\tau_H + (1/\tau_{2D} - 1/\tau_H)\frac{k_y k_z}{k^2}u_z \tag{3.4}$$

Resolution	256^3
Box size ($l_x \times l_y \times l_z$)	$2\pi \times 2\pi \times 2\pi$
Rms velocity	2.35
Viscosity	0.006
Integral length-scale ($L = 3\pi/4 \times (\int \kappa^{-1} E(\kappa) d\kappa / \int E(\kappa) d\kappa)$)	0.944
$Re = uL/\nu$	370
Dissipation (ϵ)	14.56
Dissipation scale ($\gamma = (\nu^3/\epsilon)^{1/4}$))	0.0110
$k_{max}\gamma$	1.41
Microscale Reynolds number ($R_\lambda = \sqrt{15/(\nu\epsilon)}u^2$)	72.36
Eddy turnover time ($\tau = L/u$)	0.402

TABLE 1. Turbulence characteristics of the initial velocity field. All quantities are in MKS units.

$$F_z^S = -u_z/\tau_{2D} + (1/\tau_{2D} - 1/\tau_H)\frac{k_z k_z}{k^2} u_z \tag{3.5}$$

Aside from a simple linear damping, incompressibility thus requires also a wavevector dependent contribution in order to take into account the effect of Hartmann layers. In 3.5, we see that this k-dependent contribution has exactly the same functional form as the traditional Joule damping term. It comes however with the opposite sign. When τ_{2D} and τ_J are of the same order, the traditional Joule damping can therefore be compensated by this extra term (since in general $\tau_H \gg \tau_J$) and it is thus expected that anisotropy in the parallel component will remain weak in that case. Its decay will be dominated by the simple damping term $-u_z/\tau_{2D}$ at all times.

For the perpendicular components, two phases of decay have to be distinguished. In the first one, $0 < t < \tau_{2D}$, the k-dependent terms will exert their effects. In the second one, $\tau_{2D} < t$, their influence will become negligible as u_z is damped very rapidly. In this second phase, the decay will proceed as a simple damping with characteristic time τ_H.

3.2. *Numerical results*

The set of equations we are solving are:

$$\partial_t u_i = -\partial_i(p/\rho) - u_j \partial_j u_i - \frac{A^2}{\eta}\Delta^{-1}\partial_z\partial_z u_i + F_i^S + \nu\Delta u_i, \tag{3.6}$$

where F_i^S is given by 3.3-3.5 (here $A = B/\sqrt{\mu\rho}$ denotes the Alfven velocity). These equations are solved using a pseudo-spectral code in a cubic geometry. The resolutions of our run is 256^3 Fourier modes. The initial condition for the velocity consists of a developed turbulence field that is adequately resolved in the computational domain adopted (it is obtained from a purely hydrodynamic case). Some of its characteristics are listed in table 1. In order to induce a sufficient amount of anisotropy in the flow, we have chosen a moderate value of the interaction number: $N = \tau_{tu}/\tau_J = 10$. Given the values of u and L (see Table 1), this implies that the Joule time is equal to $\tau_J = L/(uN) = 0.0402$. In this run we also assume that $\tau_{2D} = 0.0402 = \tau_J$ (looking at 2.2 this corresponds to a case where the channel width is equal to the initial $l_\perp$). From these values, one also easily computes that $Ha = 60.8$ and $\tau_H = 2.45$.

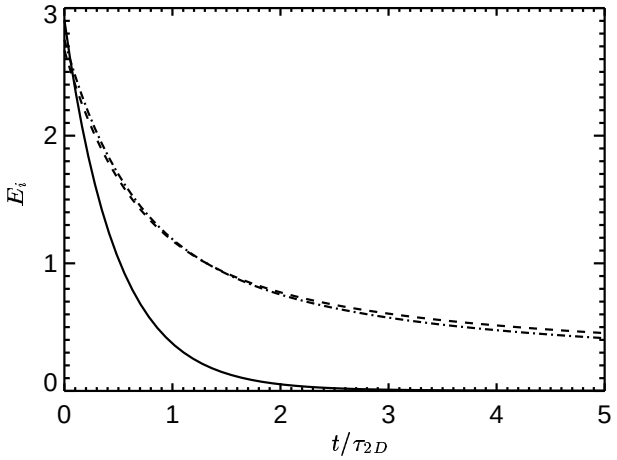

FIGURE 1. Evolution with time of the kinetic energy. Solid line: $< \|\frac{1}{2}u_z\|^2 >$; dashed line: $< \|\frac{1}{2}u_x\|^2 >$; dashed-dot line: $< \|\frac{1}{2}u_y\|^2 >$.

3.2.1. *Decay of kinetic energy*

At the beginning of the simulation all three components of the velocity field have approximately equal energy (the initial flow is isotropic). As displayed in Fig. 1, the energy of the parallel component is dissipated much faster than the one of the perpendicular components (since $\tau_{2D} \ll \tau_H$). After a time $t = 2\tau_{2D}$, the parallel component has been virtually completely dissipated.

3.2.2. *Spectra of kinetic energy*

The kinetic spectra presented in figure 2 indicate that the flow is well resolved in the simulation. A close examination shows that the slopes of the spectra for the perpendicular components tend to become steeper as time evolves, though this effect is small. The slope for the parallel direction exhibits the opposite trend and this is very marked in the different plots.

3.2.3. *Anisotropy*

To measure anisotropy we use the following diagnostics:

$$G_{ij,kl} = \frac{< (\partial_i u_j)^2 >}{< (\partial_k u_l)^2 >}. \tag{3.7}$$

They measure the relative strength of velocity gradients in different directions and for different components of the velocity field. For instance, it is easy to show that in isotropic turbulence one should have (Pope 2000):

$$G_{11,21} = G_{11,31} = 0.5,\ G_{12,22} = G_{13,33} = 2,\ G_{12,32} = G_{13,23} = 1. \tag{3.8}$$

In our simulations, the mean magnetic field is directed along the z direction (parallel direction). If the flow becomes 2D perpendicular to this direction, then one must have:

$$G_{3j,\alpha l} \to 0, \quad \text{for} \quad (j,l) \in (1,2,3) \quad \text{and} \quad \alpha \in (1,2). \tag{3.9}$$

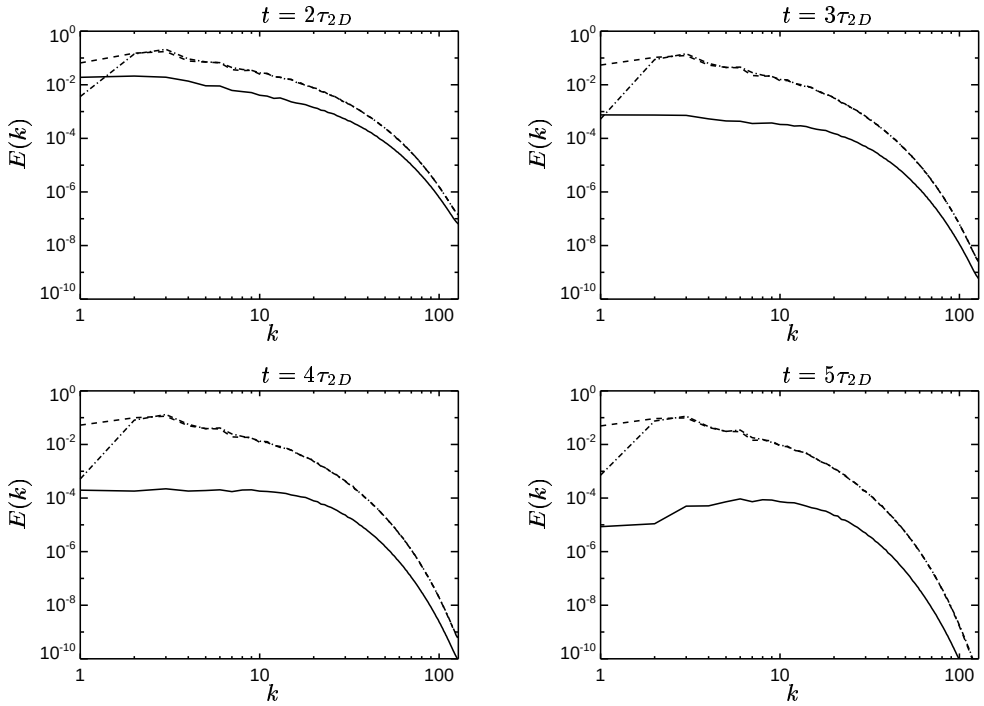

FIGURE 2. Kinetic spectra of the three velocity components at several times during the flow decay. Dashed line: u_x; dash-dot line: u_y; solid line: u_z.

In figure 3 several of the $G_{ij,kl}$ are plotted. From the figure it is clear that the symmetry $x \leftrightarrow y$ is well respected. Also, the component u_z remains significantly more isotropic than the perpendicular components with respect to this diagnostics, although with time it also evolves to a state with weaker variations along the parallel direction compared to the perpendicular directions. This behavior is well in line with the discussion contained in section 3.1.

On dimensional grounds, all the $G_{ij,kl}$ displayed in Fig. 3 should be of the order $l_\perp^2/l_\parallel^2$. Here we see that this ratio depends on the component of the velocity field considered. The ratio is larger for the parallel component than for the perpendicular components. As a consequence we see that eq. 2.1 becomes component dependent in the presence of the Hartmann damping modeling 3.3-3.5.

3.2.4. *3D visualizations of the flow*

The diagnostics presented in Fig. 3 provide a quantitative measure of the anisotropy of the flow. It is also worth to examine more qualitatively how the flow structures evolve with time. This is shown in Figs 4–6 where the energy density of the three velocity components are plotted. These plots confirm the information provided in Fig. 3: the parallel component of the velocity field remains more isotropic than the perpendicular components which become noticeably elongated in the direction of the magnetic field.

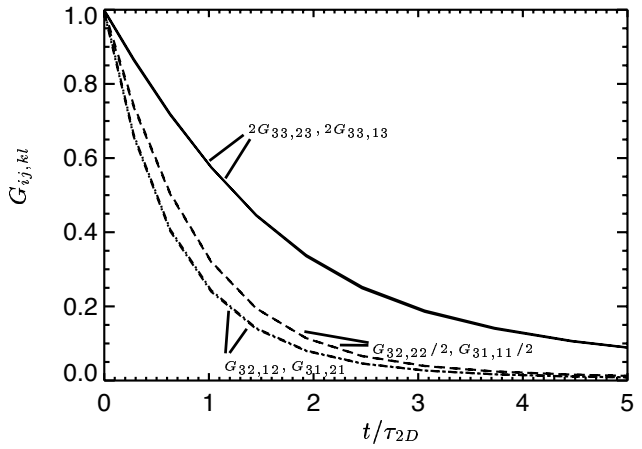

FIGURE 3. Anisotropy coefficients $G_{ij,kl}$. See figure for legend.

4. Conclusions

The idea of a pre-existing isotropic turbulence suddenly submitted to a uniform magnetic field, initially introduced by Moffatt (1967), is a purely idealized concept, since, in any experiment, during the growth of the magnetic field, eddy currents and the associated Lorentz forces are generated, which are completely neglected in section 3. In spite of this assumption, which would deserve quite a complex analysis and may be not justified at all in many experimental situations, following Moffatt and others, we focus on the mechanisms by which the homogeneous turbulence tends to become 2D and decays. Contrary to previous numerical studies on 3D homogeneous turbulence subject to a constant mean magnetic field, we try to incorporate the influence of distant Hartmann layers on the flow. The spirit behind the model introduced in section 3 is to reproduce the damping generated by the Hartmann layers though damping terms of appropriate damping times. However, to respect the incompressibility condition, wavevector dependent contribution to the model have to be considered. The effect of the model is therefore twofold. First, the velocity component parallel to the magnetic field undergoes a much more rapid damping than the perpendicular components. Less obviously, this parallel component remains largely isotropic throughout the decay due to the wavevector dependent contribution in the model.

Because of time constraints, our numerical simulations have been limited to times $0 \leq t \leq 5\tau_{2D} \ll \tau_H$. It has thus been only possible to observe the early transition from $3D$ to $2D$ turbulence. In future work, simulation runs with $t \sim \tau_H$ will be performed. These will make possible the study of typical $2D$ turbulence features like inverse energy cascade and its influence on the slope of the kinetic energy spectra.

In addition to the problem described in section 3, during the summer program, another study was started aiming at the simulation of the MATUR experiment (Messadek & Moreau 2002). This experiment, immersed in a mean applied magnetic field, uses a difference of electric potential to force a radial flow between two discs. In this system, anodes are located on one of the discs and the side wall closing the apparatus is the cathode. The MHD equations were implemented in a second-order staggered finite difference code in cylindrical coordinates. Several numerical difficulties were encountered due to the extreme thinness of the Hartmann layers which must be modeled very accurately since the whole electric current passing in the turbulent core must be close via those layers,

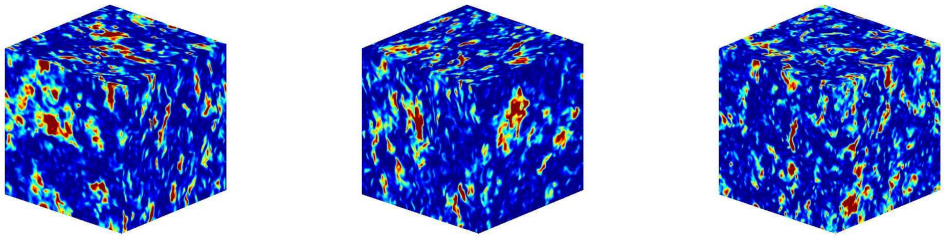

FIGURE 4. 3D visualizations of the energy density of the components of the velocity field at $t = 2\tau_J$; u_x (left), u_y (center), u_z (right). Note that the colormap of the plot corresponding to u_z is not equal to the colormap in the other two plots since the level of energy in u_z is much lower. The colormaps are not provided since the figures are meant to highlight the qualitative shapes of the turbulent structures.

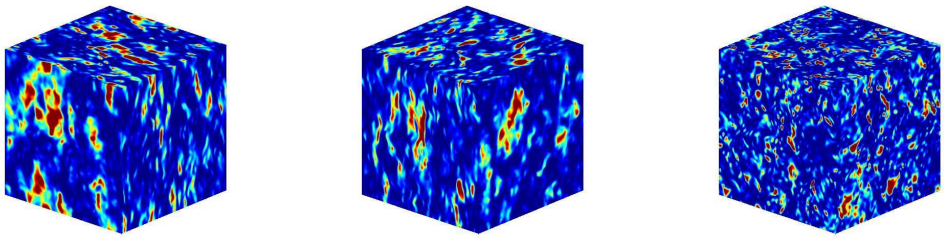

FIGURE 5. See caption of figure 4. Here $t = 3\tau_{2D}$.

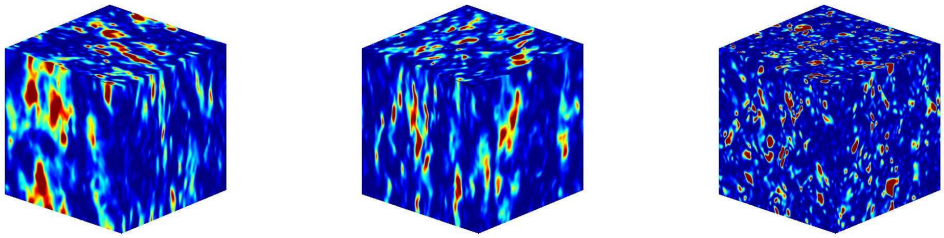

FIGURE 6. See caption of figure 4. Here $t = 5\tau_{2D}$.

which react on the core flow proportionally to the Hartmann current. As a consequence, the grid must be significantly refined in the Hartmann layers yielding very small time steps. Another important issue is the accurate representation of a series of point-like electrodes distributed on a circle at mid way between the center of the apparatus and the side wall (cathode). The difficulty here is caused by the singularities present in the experiment between the insulating parts of the Hartmann wall and the electrically conducting parts. The appropriate way to solve those difficulties without introducing any significant artifact has itself been the subject of detailed investigations. The refinement required by this set-up is very detrimental to the time step in cylindrical coordinates due

to the small radial grid-spacing at the center. To relax such a constraint and study the possibility of local refinement for both the electrodes and the Hartmann layers, current investigations have shifted to the unstructured code CDP-α developed by the ASCI program at Stanford. It is our purpose to complete this work soon and to publish the results of this benchmark in an other paper.

5. Acknowledgements

The authors are grateful to CTR for supporting this research project during the Summer Program 2004. Fruitful discussions with the other participants of the MHD session concerning this work are gratefully acknowledged.

REFERENCES

A. Alemany, R. Moreau, P. L. S. & Frisch, U. 1979 Influence of an external magnetic field on homogeneous turbulence. *J. de Mécanique* **18** (2), 275.

Branover, H. 1978 *Magnetohydrodynamic flow in ducts*. Halsted.

Davidson, P. A. 1995 Magnetic damping of jets and vortices. *J. Fluid Mech.* **299**, 153.

Davidson, P. A. 1997 The role of angular momentum in the magnetic damping of turbulence. *J. Fluid Mech.* **336**, 123.

Knaepen, B. & Moin, P. 2004 Large-eddy simulation of conductive flows at low magnetic Reynolds number. *Phys. Fluids* **16** (5), 1255.

Lee, D. & Choi, H. 2001 Magnetohydrodynamic turbulent flow in a channel at low magnetic Reynolds number. *J. Fluid Mech.* **439**, 367.

Lielausis, O. 1975 Liquid metal magnetohydrodynamics. *Atomic Energy Review* **13**, 527.

Messadek, K. & Moreau, R. 2002 An experimental investigation of mhd quasi-two-dimensional turbulent shear flows. *J. Fluid Mech.* **456**, 137.

Moffatt, H. K. 1967 On the suppression of turbulence by a uniform magnetic field. *J. Fluid Mech.* **28**, 571.

Pope, S. B. 2000 *Turbulent flows*. Cambridge University Press.

Sommeria, J. 1986 Experimental study of two-dimensional inverse energy cascade in a square box. *J. Fluid Mech.* **170**, 139.

Sommeria, J. & Moreau, R. 1982 Why, how, and when, MHD turbulence becomes two-dimensional. *J. Fluid Mech.* **118**, 507.

Tsinober, A. 1990 MHD flow drag reduction. In *Viscous drag reduction in boundary layers* (ed. D. M. Bushnell & J. N. Hefner), p. 327. AIAA Prog. Astron. Aeron. Series.

Zikanov, O. & Thess, A. 1998 Direct numerical simulation of forced mhd turbulence at low magnetic Reynolds number. *J. Fluid Mech.* **358**, 299.